

# NOISE ENHANCED SIGNAL CORRELATION AND WAVE PROPAGATION IN NETWORKS OF OSCILLATORY AND EXCITABLE SYSTEMS\*

HAUKE BUSCH AND FRIEDEMANN KAISER

Institute of Applied Physics, Darmstadt University of Technology  
Hochschulstr. 4A, 64289 Darmstadt, Germany

*(Received February 8, 2000)*

Processes in coupled nonlinear systems are discussed under the influence of external signals and noise to improve the understanding of dynamical order and function in biological systems. A network of relaxation-type oscillators with nearest-neighbour coupling is numerically investigated under the influence of exponentially correlated noise. When all oscillators are exposed to an aperiodic subthreshold signal and to spatially incoherent noise, two regimes of behaviour are observed depending on the network's coupling strength. In the case of weak coupling, noise at an intermediate level optimizes the correlation of the network oscillators with the aperiodic signal. In the case of stronger coupling the correlation with the external signal becomes lost, as intrinsic network dynamics take over. When the network is locally excited, noise-induced plane waves are built up, which move through the entire system. It is shown that the spatio-temporal pattern emerges independently of the way of the deterministic forcing. This effect may be understood as spatio-temporal stochastic resonance, since noise of an intermediate level optimizes the coherence of the wave-fronts.

PACS numbers: 87.10.+e, 5.40.Ca, 5.45.Xt

## 1. Introduction

The influence of noise is usually viewed as being detrimental to the occurrence and maintenance of regular structures, dynamical states and functional order. This widely accepted destructive role of noise has to be questioned for 20 years now, when nonlinear processes are to be taken into account. Under certain conditions, a strong constructive role of noise can be established. Noise-enhanced and noise-induced order-order and chaos-order transitions

---

\* Presented at the XII Marian Smoluchowski Symposium on Statistical Physics Zakopane, Poland, September 6–12, 1999.

have been investigated. In [1] the necessary existence of a finite dissipation in Josephson-junction elements for the occurrence of deterministic chaos is shown. Noise may have a constructive influence on the behaviour of the logistic map [2], multiplicative noise can stabilize a system by shifting the threshold of instability [3, 4]. Noise has been shown to cause a slower decay of correlations [5] and to improve predictability in a certain range of noise strength [6], when a Belousov–Zhabotinsky map is exposed to noise. With this rather arbitrary selection of some of the early investigations on the influence of noise in simple nonlinear systems we proceed to recent developments with respect to the possible constructive role of noise, mainly noise-induced or noise-enhanced processes like synchronization, coherence, amplification, information transfer and wave propagation in nonlinear systems. In general the emergence of new properties originating from the synergy of the combined action of stimuli and noise will briefly be sketched with a main emphasis on biological systems.

Fluctuations and noise are inevitable in biological systems. Whether these fluctuations can play an active role in signal detection, transfer and ordering is a question of ongoing research. Meanwhile, the constructive role of noise in signal detection and transduction is a well established fact, both theoretically and experimentally, in many cases being denoted as stochastic resonance (SR) (for reviews see [7]). This is an effect, wherein the response of a nonlinear device to a weak input signal is optimized by an intermediate level of noise. The input signal can be periodic, aperiodic, deterministically chaotic or stochastic [8]. The noise source may be white or coloured, it may be applied in an additive or multiplicative way. In the case of dichotomic, non-Markovian multiplicative noise a linear process can be sufficient [9]. SR has been observed in a variety of physical and chemical systems, including an increasing number of biological ones [10].

The constructive role of noise in elementary threshold and oscillatory devices, in excitable systems and in fluctuation driven transport is discussed in a series of papers [11]. Array-enhanced stochastic resonance and spatio-temporal synchronization has been proven to occur in arrays of bistable elements [12, 13]. In [14] it is shown that a SR kind of behaviour amplifies an external, periodic signal and enhances its transfer through a system of coupled oscillators. Noise-induced synchronization of coupled excitable systems has been reported in [15]. Noise-sustained pulsating patterns and global oscillations have been observed in an array of activator–inhibitor elements, where spatially uncorrelated noise acts parametrically on the threshold of the excitable system [16].

The ability of noise to enhance spatio-temporal patterns and to increase some coherent or collective dynamical properties may be viewed as a generalization of the notion of stochastic resonance to spatially extended sys-

tems. The phenomenon of spatio-temporal stochastic resonance (STSR) was first observed by Jung and Mayer–Kress in a noisy cellular automata system [17]. STSR has been further observed experimentally in noise-induced  $\text{Ca}^{2+}$ -waves [18] and in noise-supported travelling waves in a chemical reaction [19].

So far most studies were concerned with either noise-induced signal amplification and synchronization or noise-induced pattern formation. The question we study in this paper is how noise can enhance both signal-detection and the formation of a spatio-temporal pattern within one system. As a working model we investigate the response of a rectangular lattice of relaxation-type oscillators with nearest-neighbour coupling to a subthreshold aperiodic input signal under the influence of spatially coherent and incoherent noise. We show that the system’s behaviour can change from coupling-enhanced aperiodic stochastic resonance (ASR) to noise-assisted synchronization of the network by raising the global network coupling strength, thus combining noise-assisted signal detection, synchronization and wave propagation. It is shown that the latter can be characterized as some type of spatio-temporal stochastic resonance.

The paper is organized as follows. The working model is introduced in Section 2. In Section 3, we discuss the numerical results for two different realizations of the network models and show that they can exhibit both aperiodic and spatio-temporal stochastic resonance. The paper is concluded in Section 4.

## 2. Model

A two-dimensional  $m \times n$  array, whose elements consist of noisy relaxation-type nonlinear oscillators, is investigated. The only requirement for the oscillators used is their ability to perform transitions from a fixed point to a limit cycle, when driven by both a deterministic and a noisy signal. The oscillators’ dynamics have to be determined by a slow recovery process and a large amplitude of the fast variable. Many other oscillator models exhibit this behaviour, *e.g.* the well-known FitzHugh–Nagumo model and some others [20].

The network is described by the following set of coupled differential equations:

$$\varepsilon \frac{dx_{ij}}{dt} = y_{ij} - \frac{x_{ij}^2}{2} - \frac{x_{ij}^3}{3}, \quad (1)$$

$$\begin{aligned} \frac{dy_{ij}}{dt} = & \alpha - x_{ij} - q(x_{i-1,j} + x_{i+1,j} + x_{i,j-1}) \\ & - \mu_{ij} x_{\text{ext}} + \xi_{\text{coh}}(t) + \xi_{ij}(t), \end{aligned} \quad (2)$$

with  $i \leq n$  being the row and  $j \leq m$  being the column index.  $x_{ij}$  and  $y_{ij}$  are the fast and the slow recovery variables, respectively. Nearest-neighbour coupling to only three neighbours is introduced via the coupling constant  $q$ . Eq.(2) has no back coupling  $qx_{i,j+1}$ . Hence, excitation can propagate only in one direction, that is towards higher column indices (from  $j - 1$  to  $j$ ). With this assumption we want to realize the fact that many processes in biological systems exhibit a sense of direction, *e.g.* in afferent and efferent nervous signalling [21].

Each uncoupled oscillator exhibits stable foci for  $|\alpha+0.5| > 0.5, \alpha(1+\alpha) < 2\sqrt{\varepsilon}$  and a Hopf-bifurcation at  $\alpha = 0$  [22]. An external, periodically driven oscillator of the same kind is coupled to the network to generate an aperiodic signal [23], which is globally fed into the network via the coupling constant  $\mu_{ij}$

$$\varepsilon \frac{dx_{\text{ext}}}{dt} = y_{\text{ext}} - \frac{x_{\text{ext}}^2}{2} - \frac{x_{\text{ext}}^3}{3}, \quad (3)$$

$$\frac{dy_{\text{ext}}}{dt} = -x_{\text{ext}} + \alpha + A \cos(\omega t). \quad (4)$$

The noise terms appearing in the model equation (2) include spatially incoherent noise sources ( $\xi_{ij}(t)$ ), *i.e.* the noise is uncorrelated from site to site, and spatially coherent noise ( $\xi_{\text{coh}}(t)$ ). These two noise sources can act on each system oscillator. The numerical simulations use exponentially correlated, coloured noise for both  $\xi_{ij}$  and  $\xi_{\text{coh}}$

$$\langle \xi(t) \rangle = 0, \quad (5)$$

$$\langle \xi(t)\xi(t') \rangle = \frac{\sigma^2}{\tau_c} \exp\left(-\frac{|t-t'|}{\tau_c}\right), \quad (6)$$

where  $\tau_c$  is the noise correlation time and  $\sigma^2$  the variance of the Gaussian-distributed noise amplitudes. Here,  $\sigma$  refers to the intensities of both the spatially incoherent ( $\sigma_{\text{inc}}$ ) as well as the spatially coherent ( $\sigma_{\text{coh}}$ ) noise terms.  $\xi_{ij}(t)$  and  $\xi_{\text{coh}}(t)$  are generated through a higher-dimensional Ornstein-Uhlenbeck process using an integral algorithm as described in [24]. The generating equation reads

$$\dot{\xi}(t) = \frac{1}{\tau_c}(-\xi(t) + \eta(t)), \quad (7)$$

with  $\eta(t)$  being some Gaussian, white noise. Application of coloured noise is preferred, because it provides a more realistic description of real fluctuations in biological systems, as compared to spectrally flat noise. Although the functional significance of the colour of the noise still remains elusive [25], it

has nevertheless been observed in biological systems [26]. The question as to whether coloured noise can reduce or improve SR is a matter of ongoing research since the appearance of an excellent paper on this topic [27].

Throughout this paper we use the following set of common parameters:  $\varepsilon = 0.01$ ,  $\alpha = 0.1$ ,  $A = 1.0$ ,  $\omega = 18s^{-1}$ ,  $\tau_c = 0.01$ . The cosine signal drives the input oscillator into a chaotic state and the coupling constants  $\mu_{ij}$  and  $q$  are adjusted in such a way that the array oscillators yield stable foci in the absence of noise. The differential equations are integrated numerically using a 5th-order Runge–Kutta algorithm [28]. Network simulations are run with an integration stepsize of  $\Delta t = 3.49 \times 10^{-3}$ s. Control runs with smaller time steps and larger networks led to the same results.

### 3. Results

For sufficiently large coupling strength  $q$ , an excited array element will be the nucleus of excitatory waves spreading through the entire network. Here, by means of the broken symmetry within the nearest-neighbour coupling, the creation of plane-waves is observed, only. In the following, we refrain ourselves to values of  $q$ , below which excitation of the array elements cannot be sustained through local excitation. We investigate the effect of the noise intensity  $\sigma$  and the coupling strength  $q$  on the response of the network to the aperiodic input signal. The correlation between the response and the input signal is calculated using the powernorm  $C_0$  [29]. Here,  $C_0$  is defined in the following way:

$$C_{\text{ext}} = \frac{1}{N} \sum_{i,j}^{m,n} \langle (x_{ij} - \langle x_{ij} \rangle_t)(x_{\text{ext}} - \langle x_{\text{ext}} \rangle_t) \rangle_t, \quad (8)$$

where  $\langle \rangle_t$  denotes time averaging and the sum extends over all  $N = m \times n$  network elements. For calculating the correlation between network elements,  $C_0$  can be written as:

$$C_{\text{int}} = \binom{N}{2}^{-1} \sum_{\{ij, i'j'\}} \langle (x_{ij} - \langle x_{ij} \rangle_t)(x_{i'j'} - \langle x_{i'j'} \rangle_t) \rangle_t, \quad (9)$$

where  $\langle \rangle_t$  denotes time averaging. The sum extends over all  $\binom{N}{2}$  different combinations of  $ij$  with  $i'j'$ , where  $\binom{N}{2}$  is the binomial coefficient and  $N$  the number of array elements.

Note that stochastic resonance is associated with optimal input–output signal coherence as well as signal amplification. In order to account for the latter effect we use non-normalized correlation measures.

### 3.1. Noise-enhanced input-output correlation

For our investigation we take  $m = n = 8$  and apply periodic boundary conditions. The coherent noise term is zero ( $\sigma_{\text{coh}} = 0$ ). We choose  $\mu_{ij} = 0.20 \forall i, j$ , thus all 64 oscillators are driven by the same external signal  $x_{\text{ext}}$ . Figs. 1(a) and (b) show the absolute value of  $C_{\text{ext}}$  and  $C_{\text{int}}$  as a function of  $q$  and  $\sigma_{\text{inc}}$ . Dark colours correspond to high values of the powernorm. Figs. 1(c) and (d) depict a cross-section of the contour plots at  $\sigma_{\text{inc}} = 0.008$ .

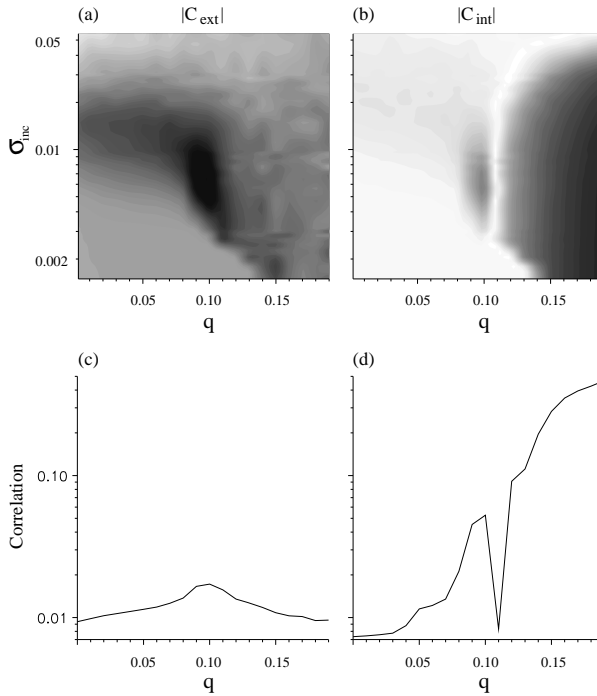


Fig. 1. Contour plots of the absolute values of (a)  $|C_{\text{ext}}|$  and (b)  $|C_{\text{int}}|$  as a function of the coupling strength  $q$  and noise intensity  $\sigma_{\text{inc}}$ . The array size is  $m = n = 8$ . All oscillators are externally driven. The correlation values are linearly greyscale-coded in 60 steps from 0 up to 0.017 in (a) and up to 0.50 in (b). Data points were obtained in triplicate by averaging over 15000 periods of the periodic driver. Figures (c) and (d) show a cross-section of  $|C_{\text{ext}}|$  and  $|C_{\text{int}}|$  at  $\sigma_{\text{inc}} = 0.008$ , respectively. Other parameters:  $\sigma_{\text{coh}} = 0$  and  $\mu_{ij} = 0.20$ .

Figs. 1(a) and (c) reveal that there is an intermediate range of the noise intensity and coupling strength around  $\sigma_{\text{inc}} = 0.008$  and  $q = 0.10$ , for which the correlation  $C_{\text{ext}}$  is maximal. Here, the response of the network most closely resembles the input signal. Note that the embedding of the oscil-

lators in a network raises the ASR-induced correlation almost by a factor of two. The absolute maximum at  $q = 0.10$  is  $C_{\text{ext}} = 0.017$ , whereas the local maximum for  $q = 0$ , when all network oscillators act as independent excitable systems, is  $C_{\text{ext}} = 0.009$ .

This behaviour is reflected by the time series of one sample oscillator of the network [Figs. 2(b) and (c)]. The input signal remains the same [Fig. 2(a)], but the coupling strength  $q$  increases from (b)–(d). The noise intensities are chosen to optimize the network’s capability as a detector for the aperiodic spike sequences of the input oscillator. If  $q$  is small [Fig. 2(b)], there are few response relaxation oscillations (spiking events) to the input signal from (a). Raising the coupling strength leads into a parameter region, wherein the aperiodicity of the input as well as the variation of the oscillation amplitudes is rendered the most clearly [Fig. 2(c)]. A further increase of the coupling strength exhibits a regime of noise-induced oscillations, whose

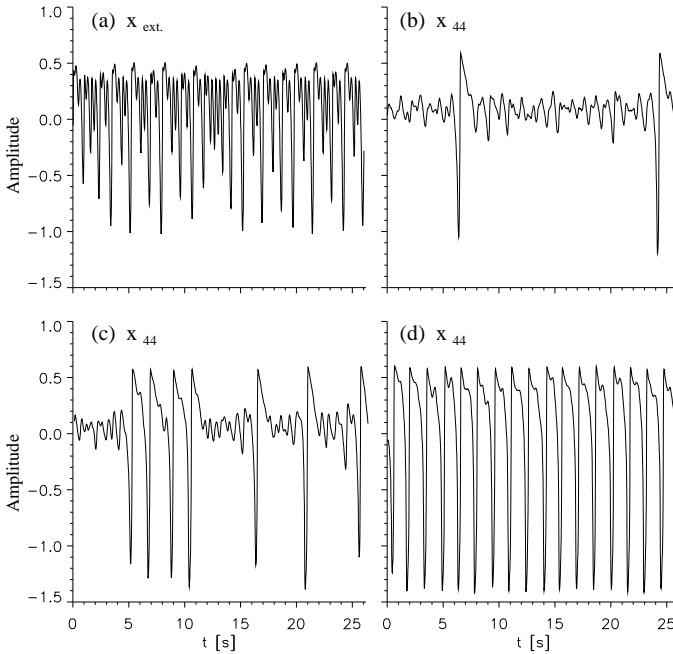


Fig. 2. Time series of the oscillators. (a) Time series of the external oscillator ( $x_{\text{ext}}$ ), which is driven into a chaotic regime by appropriate forcing. This aperiodic signal is globally coupled into the network. (b)–(d) Response of one sample network oscillator ( $x_{44}$ ) at three different coupling strengths in the regime of optimized, noise-induced response. All time series show the response to the same aperiodic input signal from (a). Parameter values: (b)  $q = 0.01$ ,  $\sigma_{\text{inc}} = 0.01$ , (c)  $q = 0.1$ ,  $\sigma_{\text{inc}} = 0.008$ , (d)  $q = 0.20$ ,  $\sigma_{\text{inc}} = 0.01$ . Other parameters are the same as in Fig. 1.

amplitude and frequency are determined by the intrinsic dynamical properties of the coupled oscillators, nearly independent of the aperiodic input signal [Fig. 2(d)].

As a consequence of the regular network oscillations the correlation  $C_{\text{ext}}$  starts to decline for  $q > 0.10$  for all values of  $\sigma_{\text{inc}}$ , when a transition from a noise-enhanced input–output correlation to a noise-induced array synchronization takes place, which can be seen from  $C_{\text{int}}$  [Figs. 1(b) and (d)]. The local maximum of  $C_{\text{int}}$  around  $q = 0.10$  corresponds to the absolute maximum of  $C_{\text{ext}}$  in Figs. 1(b) and (c), thus revealing the ASR-induced correlation between the network oscillators. Raising the coupling strength further leads to a small parameter region, in which  $C_{\text{int}}$  tends to zero. Here, the network’s ability to detect temporal patterns is reduced, whereas a global phase synchronization of the network oscillators has not yet been established. The network shows patchy pulsating patterns, *i.e.* temporally and spatially changing areas of activity, which result in a loss of the network-internal correlation  $C_{\text{int}}$ . For stronger coupling  $q$ , the intrinsic noise starts to dominate over the influence of the aperiodic input signal and the resulting phase synchronization between network oscillators causes the buildup of a spatio-temporal pattern, thus strongly increasing the inner network correlation  $C_{\text{int}}$ .

The dependency on  $q$  can be explained by the fact, that the network coupling lowers the effective threshold of each oscillator. The regular oscillations are hence a noisy precursor of the completely synchronized oscillations that occur for  $q > 0.25$  in the deterministic case.

### 3.2. Combined influence of spatially coherent and incoherent noise sources

The combined influence of different noise sources reveals the fact that each subsystem (excitatory/oscillatory unit) may be influenced by both spatially coherent noise (*e.g.* an external noisy signal acting on the whole system) and spatially incoherent noise (*e.g.* thermal background or environment). In [30] it has been shown that internal (spatially uncorrelated) noise plays a constructive role in information transfer through ion channels via an increase in external (*i.e.* spatially correlated) noise. In [14] both a constructive and destructive influence of the combined noise sources has been demonstrated.

In our investigation we expose all array oscillators to spatially incoherent and coherent noise sources, whose intensities are denoted as  $\sigma_{\text{inc}}$  and  $\sigma_{\text{coh}}$ , respectively. The inner network coupling strength is set to  $q = 0.10$ . Fig. 3 depicts a contour plot of the resulting correlation values of  $C_{\text{ext}}$ . The correlation can be maximized by both  $\xi_{\text{coh}}$  or  $\xi_{ij}$ , individually. The maximal correlation induced by the coherent noise ( $C_{\text{ext}} = 0.007$ ) is about two

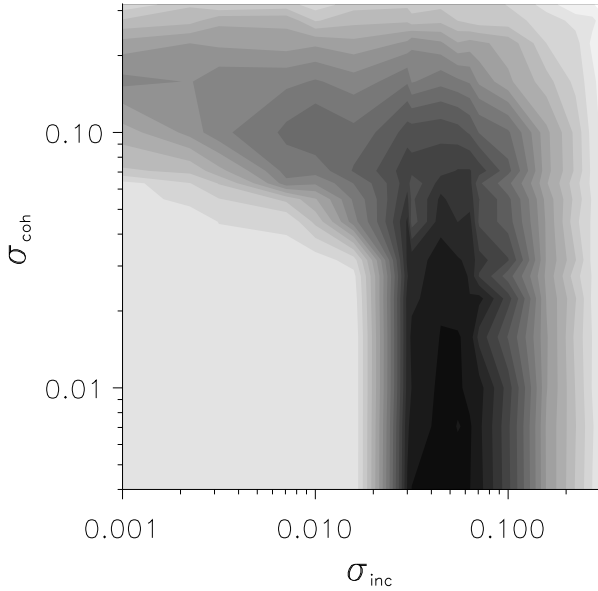


Fig. 3. Contour plot of  $|C_{\text{ext}}|$  in case of the network being exposed to both spatially coherent ( $\sigma_{\text{coh}}$ ) and incoherent ( $\sigma_{\text{inc}}$ ) noise of varying intensity. The correlation values are linearly greyscale-coded in 20 steps from 0 up to 0.017. Data points were obtained in triplicate by averaging over 15000 periods of the periodic driver. Other parameters:  $q = 0.10$ ,  $\tau_{\text{inc}} = \tau_{\text{coh}} = 0.01$ .

times smaller than the maximum caused by  $\xi_{ij}$  ( $C_{\text{ext}} = 0.017$ ). Raising  $\sigma_{\text{inc}}$  results in an increase of  $C_{\text{ext}}$ , as can be seen for  $\sigma_{\text{coh}} \approx 0.15$ . The system thus benefits from the addition of incoherent noise, but not *vice versa*, because  $C_{\text{ext}}$  is maximized in the absence of the coherent noise term. The addition of spatially coherent noise lowers the correlation. These findings suggest, that there is no cooperative effect between spatially incoherent and coherent noise in this system considered. The influence of the different noise sources on  $C_{\text{ext}}$  is simply additive. The reason for this lies in the fact that  $\xi_{\text{coh}}$  and the coupling via  $q$  force nearest neighbours in the network into different directions. The coherent noise source drives all oscillators in the same direction (*i.e.* either further into the stable regime or towards the threshold), whereas the coupling drives neighbouring oscillators in opposite directions, due to the negative sign of the coupling constant  $q$  (Eq. 2). Thus, these two forces are counteracting.

It should be remarked that all the results presented are also valid for free boundary conditions.

### 3.3. Noise enhanced wave propagation

In the last part of this chapter it is shown that the system exhibits a spatio-temporal stochastic resonance-type of behaviour in the region of synchronized network oscillations. As an example we present results for a rectangular lattice ( $m = 132, n = 32$ ), apply free boundary conditions and set  $q = 0.15$ . The coherent noise term is switched off ( $\sigma_{\text{coh}} = 0$ ). We choose  $\mu_{ij} = 0$  except for  $j = 1$  and  $i = 15, 17$ . By only exciting two oscillators one can simulate a rather general triggering of the network.

The effect of varying the noise intensity  $\sigma_{ij}$  can be seen from Fig. 4 (a)–(d). In the case of low noise intensity, the system remains quiescent [Fig. 4(a)] except for the two elements on the far left that are determinis-

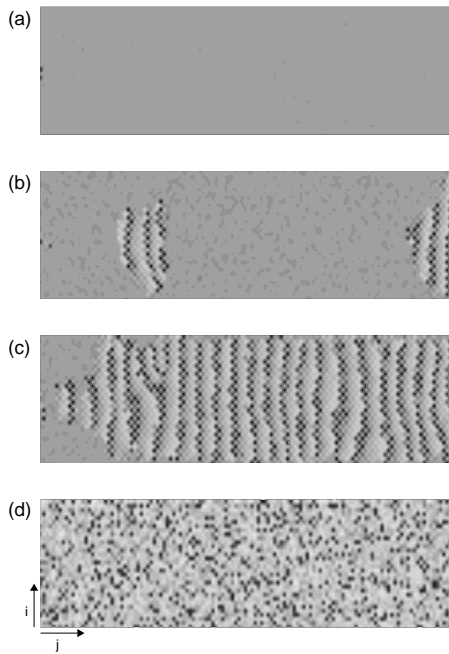


Fig. 4. Snapshots of an  $32 \times 128$  array of oscillators under the influence of spatially incoherent noise. Noise intensity increases from (a)–(d). Two elements in the first column are deterministically driven by an external oscillator. This generates an aperiodic triggering of the network. The system is initially at rest. The snapshots are taken after a transient of 2000 driving periods. The amplitude values increase in 60 steps from  $-1.5$  to  $+1.0$ , whereas dark spots denote the negative deflections, white spots the positive overshoot (cf. Fig. 2). Parameter values: (a)  $\sigma_{\text{inc}} = 0.001$ , (b)  $\sigma_{\text{inc}} = 0.0055$ , (c)  $\sigma_{\text{inc}} = 0.008$ , (d)  $\sigma_{\text{inc}} = 0.03$ . Other parameters:  $\mu_{ij} = 0$  except for  $\mu_{15,1} = \mu_{17,1} = 0.25$  and  $\sigma_{\text{coh}} = 0$ .

tically driven. Increasing the level of noise slightly results in small patches of activity that slowly move from left to right through the entire network [Fig. 4(b)]. Fig. 4(c) presents the regime of an optimal noise level, at which plane wave-fronts of excitation move steadily from left to right through the whole system. Raising the noise intensity further results in the breakup of the wave-fronts and in independent, noise-dominated oscillations of the network elements [Fig. 4(d)].

Please note the structure of the wave-fronts, in which every second element pulses in phase, whereas direct neighbours oscillate in an anti-phase manner [Figs. 4(b)–(c)]. This is caused by a combinatory effect of the nearest-neighbour coupling between elements within one column (Eq. 2) and the elements' oscillatory behaviour. Figs. 2(a)–(d) show how the  $x_{ij}$ -variables change their sign during one oscillation cycle. Coupling and noise then force the oscillators to drive each other into the fixed or excited state in a temporal and spatial alternating fashion. The result is a phase-locked oscillatory behaviour within one column of the array. The phase synchronization finally extends noise-assisted across the entire network by means of the unidirectional coupling.

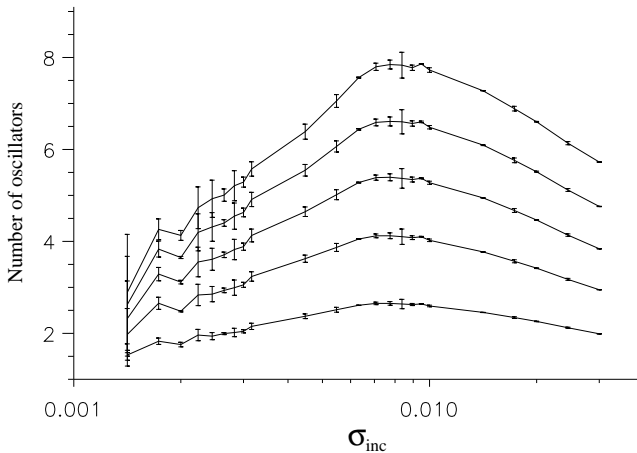


Fig. 5. Plot of the array- and time-averaged ( $16 \leq j \leq 128$ ) number of oscillators per column spiking within a time interval  $\Delta t$ .  $\Delta t$  increases from  $\Delta t = 0.1s$  to  $\Delta t = 0.5s$  from bottom to top in intervals of  $0.1s$ . A spike is counted when an oscillator crosses a threshold of  $x_{th} = -0.5$  from above. Data points have been obtained in triplicate with time series running over 15000 forcing cycles each. The recording of spike events started after a transient of 1000 forcing cycles of the cosine driver. Error bars represent standard deviations. Other parameters are the same as in Fig. 4.

The propagation speed of the plane wave-fronts within an active zone is fairly independent of the noise intensity applied, mainly because the relaxation oscillations are robust against fluctuations added to them. So each element oscillates with a frequency of  $\nu \approx 0.62\text{s}^{-1}$ .

A way of quantifying STSR in the above system is to calculate the average number of oscillators within each column of the array that are spiking within a short time interval  $\Delta t$ . Fig. 5 reveals that this quantity is maximized at a finite level of noise. The maxima become more pronounced with longer time intervals  $\Delta t$ , whereas their positions remain unchanged. This means that the oscillations of the array elements within one column are the most synchronized around  $\sigma_{\text{inc}} \approx 0.008$ , *i.e.* that the wave-fronts are the most coherent for this intermediate noise intensity.

#### 4. Conclusions

In this study a two-dimensional array of excitable systems under the influence of an external signal together with spatially incoherent and coherent noise is discussed. The system models some aspects of neuronal action potential dynamics and signalling in a noisy environment. The above simulations lead to the conclusions that the ordering role of noise can be used by the system in two ways, depending on its excitability.

Weak network coupling strength, *i.e.* low excitability, shows a noise-enhanced sensitivity towards a subthreshold, aperiodic input signal. The excitable foci of the network oscillators are collectively capable of detecting temporal patterns of the signal. This behaviour can thus be regarded as some kind of frequency encoding and network-enhanced aperiodic stochastic resonance. The conditions leading to ASR are very general, as the input signal varies on a time scale that is comparable to the characteristic time of the responding network.

Raising the network coupling strength, which is equivalent to lowering the network elements' effective thresholds, results in a different network behaviour. External signals merely serve as a trigger for excitation, whereas the global dynamics of the system are determined by the intrinsic properties of the individual network oscillators. Feedback coupling causes a mutual inhibition of neighbouring array elements that leads to a synchronizing effect. This is the reason for the noise-assisted buildup of a spatio-temporal pattern of plane wave-fronts moving in the direction given by the unidirectional coupling. The roughness of the wave-fronts can be optimized by an intermediate level of noise. This suggests a kind of spatio-temporal stochastic resonance behaviour as shown by calculating the average number of synchronously oscillating array elements. The transition between the above described regimes of behaviour can be discerned clearly through the loss of inner-network coherence despite increasing coupling strength [Fig. 1 (c),(d)].

Finally it is worth mentioning, that the optimal noise strengths for both noise-induced input–output correlation and noise-induced wave propagation are the same. Which of the phenomena are predominant depends on the coupling strength  $q$  and therefore on the height of the threshold barrier of the array oscillators, only.

Although this model is far from simulating real neural processes, it nevertheless suggests a noise-assisted mechanism, how neural networks in the brain could switch from individual signalling to a global, coherent pulsing that is controlled by the intrinsic features of the neurons and sustained through noise, regardless of an external signal. Such a transition to a synchronized state could be mediated by altering the neurons' excitability, *e.g.* through a lowered firing threshold. The regime of coherent oscillations is reminiscent of the synchronous discharges of neurons in epileptic seizures, whereas the constructive role of noise in the brain and the level of inhibitory or excitatory coupling between neurons still is a matter of ongoing experimental research. Quite general, it remains an open question, whether biological systems have any functional benefit in applying noise-enhanced signal propagation and detection, though it could be shown in several biological systems that the process of SR can work [31]. A first demonstration that noise-enhanced sensory dynamics can lead to improved functional behaviour has been shown quite recently [32].

## REFERENCES

- [1] B.A. Hubermann, J.P. Crutchfield, N.H. Packard, *Appl. Phys. Lett.* **37**, 750 (1980).
- [2] G. Mayer-Kress, H. Haken, *J. Stat. Phys.* **26**, 149 (1981).
- [3] R. Graham, A. Schenzle, *Phys. Lett.* **A26**, 1676 (1982).
- [4] G.V. Welland, F. Moss, *Phys. Lett.* **A89**, 273 (1982).
- [5] H.P. Herzel, W. Ebeling, *Phys. Lett.* **A111**, 1 (1985).
- [6] H.P. Herzel, W. Pompe, *Phys. Lett.* **A122**, 121 (1987).
- [7] K. Wiesenfeld, F. Moss, *Nature* **373**, 33 (1995); L. Gammaitoni, P. Hänggi, P. Jung, F. Marchesoni, *Rev. Mod. Phys.* **70**, 223 (1998).
- [8] F. Moss, D. Pierson, D. O'Gorman, *Int. J. Bifurcation and Chaos* **4**, 1 (1994); J.J. Collins, T.T. Imhoff, G. Griegg, *Phys. Rev.* **E52**, R3321 (1995); D. Chialvo, A. Longtin, J. Müller-Gerking, *Phys. Rev.* **E55**, 1798 (1997); R. Castro, T. Sauer, *Phys. Rev. Lett.* **79**, 1030 (1997); A. Silchenko, T. Kapitaniak, V. Anishchenko, *Phys. Rev.* **E59**, 1593 (1999).
- [9] A. Fulinsky, *Phys. Rev.* **E52**, 4523 (1995).

- [10] J.K. Douglass, L. Wilkens, E. Pantazelou, F. Moss, *Nature* **365**, 337 (1993); J. Levin, J. Miller, *Nature* **380**, 165 (1996); J.J. Collins, T.T. Imhoff, G. Griegg, *J. Neurophysiol.* **76**, 642 (1996); P. Cordo, J.T. Inglis, S. Verschueren, J.J. Collins, D.M. Merfeld, S. Rosenblum, S. Buckley, F. Moss, *Nature* **383**, 769 (1996); B.J. Gluckman, T.I. Netoff, E.J. Neel, W.L. Ditto, M.L. Spano, S.J. Schiff, *Phys. Rev. Lett.* **77**, 4098 (1996); S.M. Bezurkov, I. Vodyanoy, *Nature* **385**, 319 (1997); S.M. Bezurkov, I. Vodyanoy, *Biophys. J.* **73**, 2456 (1997); J.J. Collins, T.T. Imhoff, G. Griegg, *Phys. Rev.* **E56**, 923 (1997).
- [11] *Chaos* **8**, 539 (1998).
- [12] J. Lindner, B. Meadows, W. Ditto, M. Inchiosa, A.R. Bulsara, *Phys. Rev. Lett.* **75**, 3 (1995).
- [13] A. Neiman, L. Schimansky-Geier, F. Moss, B. Shulgin, J.J. Collins, *Phys. Rev.* **E60**, 284 (1999).
- [14] C. Hauptmann, F. Kaiser, C. Eichwald, *Int. J. Bifurcation and Chaos* **9**, 1159 (1999).
- [15] J. Pham, K. Pakdaman, J.-F. Vilbert, *Phys. Rev.* **E58**, 3610 (1998).
- [16] H. Hempel, L. Schimansky-Geier, J. García-Ojalvo, *Phys. Rev. Lett.* **82**, 3713 (1999).
- [17] P. Jung, G. Mayer-Kress, *Phys. Rev. Lett.* **74**, 2130 (1995).
- [18] P. Jung, A. Cornell-Bell, K.S. Madden, F. Moss, *J. Neurophysiol.* **79**, 1098 (1998).
- [19] S. Kádár, J. Wang, K. Showalter, *Nature* **391**, 770 (1998).
- [20] F. Kaiser, *Cell. Mol. Biol. Lett.* **4**, 87 (1999).
- [21] E. Başar, H. Flohr, H. Haken, A.J. Mandell, *Synergetics of the Brain*, Springer-Verlag, Berlin 1983.
- [22] B. Braaksma, J. Grasman, *Physica* **D68**, 265 (1993).
- [23] C. Eichwald, J. Walleczek, *Phys. Rev.* **E55**, R6315 (1997).
- [24] R.F. Fox, J.R. Gatland, R. Roy, G. Vemuri, *Phys. Rev.* **A38**, 5938 (1988).
- [25] D. Nozaki, D.J. Mar, P. Grigg, J.J. Collins, *Phys. Rev. Lett.* **82**, 2402 (1999).
- [26] Y. Yamamoto, R. Hughson, *Physica* **D68**, 250 (1993).
- [27] P. Hänggi, P. Jung, C. Zerbe, F. Moss, *J. Stat. Phys.* **70**, 25 (1993).
- [28] W. Press, S. Teukolsky, W. Vetterling, B. Flannery, *Numerical Recipes in Fortran*, Cambridge Univ. Press, Cambridge 1992.
- [29] C. Henegan, J.J. Collins, C.C. Chow, T.T. Imhoff, S.B. Lowen, M.C. Teich, *Phys. Rev.* **E54**, R2228 (1996).
- [30] P.C. Gailey, A. Neiman, J.J. Collins, F. Moss, *Phys. Rev. Lett.* **79**, 4701 (1997).
- [31] J.J. Collins, *Nature* **402**, 241 (1999).
- [32] D.F. Russell, L.A. Wilkens, F. Moss, *Nature* **402**, 291 (1999).